CrossMark

Chemical reaction effect on MHD viscoelastic fluid over a stretching sheet through porous medium

M. K. Nayak

Abstract The heat and mass transfer effects in a boundary layer flow through porous medium of an electrically conducting viscoelastic fluid subject to transverse magnetic field in the presence of heat source/sink and chemical reaction have been analyzed. It has been considered the effects of radiation, viscous and Joule dissipations and internal heat generation/absorption. Closed form solutions for the boundary layer equations of viscoelastic, second-grade and Walters' B' fluid models are obtained. The method of solution involves similarity transformation. The transformed equations of thermal and mass transport are solved by applying Kummer's function. The solutions of temperature field for both prescribed surface temperature as well as prescribed surface heat flux are obtained. It is important to remark that the interaction of magnetic field is found to be counterproductive in enhancing velocity and concentration distribution whereas the presence of chemical reaction as well as porous matrix with moderate values of magnetic parameter reduces the temperature and concentration fields at all points of flow domain.

List of symbols

α	Thermal diffusivity
k	Thermal conductivity
R_c	Viscoelastic parameter
P_r	Prandtl number
S_c	Schmidt number
T	Non-dimensional temperature
t	Non-dimensional time
ρ	Density of the fluid
υ	Kinematics coefficient of viscosity
σ	Electrical conductivity
R	Radiation parameter
E_c	Eckert number
C_f	Skin friction coefficient
k_0	Modulus of the viscoelastic fluid
m_w	Rate of mass flux
k_1	Mean absorption coefficient
K_p	Permeability parameter
M_n	Magnetic parameter
B_0	Magnetic field strength
Q	Heat source/sink parameter
T'	Temperature of the field
p	Pressure
D	Molecular diffusivity
q_r	Radiative heat flux
σ^*	Stefan–Boltzmann constant
C_p	Specific heat

M. K. Nayak (✉)
Department of Physics, Radhakrishna Institute of
Technology and Engineering, Bhubaneswar, Odisha, India
e-mail: mkn2122@gmail.com

q_w	Wall heat flux
τ_w	Wall shear stress
T_∞	Temperature far from sheet
T_w	Wall temperature
K_c	Chemical reaction parameter
A, B, E_0, E_1	Constants

1 Introduction

The importance of fluid flow over a stretching sheet can be perceived for its ever increasing inevitable applications in industries and in contemporary technology. The applications of the stretching sheet problem are such as polymer sheet extrusion from a dye, drawing, thinning and annealing of copper wires, glass fiber and paper production, the cooling of a metallic plate in a cooling bath etc. The production of these sheets requires that the melt issues from a slit and is stretched to get the desired thickness. The final product depends on rate of cooling in the process and the process of stretching. Sakiadis [1] was first to study the boundary-layer behavior on a continuous solid surface moving with constant speed. Crane [2] was the first to achieve an elegant analytical solution to the boundary layer equations for the problem of steady two-dimensional flow through a stretching surface in a quiescent incompressible fluid.

The growing need for chemical reaction and hydrometallurgical industries needs the study of heat and mass transfer with chemical reaction. There are numerous transport processes that are governed by the combined action of buoyancy forces due to both thermal and mass diffusion in the presence of chemical reaction effect. These processes occur in the nuclear reactor safety and combustion systems, solar collectors, metallurgical and chemical engineering etc.

Khan and Sanjayanand [3] reported an analytical solution of the viscoelastic boundary layer flow and heat transfer over an exponentially stretched sheet considering the viscous dissipation in the heat transport equation. Kar et al. [4] investigated the heat and mass transfer effects on a dissipative and radiative viscoelastic MHD flow over a stretching porous sheet. Nayak et al. [5] analyzed the effects of chemical reaction on MHD flow of a viscoelastic fluid through porous medium.

Stagnation point flow is important because stagnation point appears in virtually all flow fields in science and engineering. The stagnation-region encounters the highest pressure, heat transfer and rates of mass diffusion. This problem has been studied extensively by Hayat et al. [6] and widely studied in several situations recently on account of the importance of its applications in industries and manufacturing processes.

Bataller [7] investigated the effect of thermal radiation on heat transfer in a boundary layer viscoelastic second order fluid over a stretching sheet with internal heat source/sink. Recently, Hayat et al. [8] studied the effects of chemical reaction of unsteady three dimensional flow of couple stress fluid over a stretching surface. Gireesha et al. [9] have studied the boundary-layer flow and heat transfer of a dusty fluid flow over a stretching sheet in presence of non-uniform heat source/sink and radiation. Parsa et al. [10] investigated the MHD boundary-layer flow over a stretching surface with internal heat generation or absorption. But these studies are confined to hydrodynamic flow and heat transfer in Newtonian fluids. However, most of the practical situations demand non-Newtonian fluids which are extensively used in many industrial and engineering applications.

Mustafa et al. [11, 12] studied the boundary layer flow as well as axisymmetric flow of nano fluid over a non-linearly stretching sheet. A common feature of the above investigations is that nano fluids can impart dramatic improvements in the thermal conductivity of host fluids compared to that of traditional fluids. This further leads to enhance the heat transfer and viscosity.

Raptis [13] studied the heat transfer in a viscous fluid over a stretching sheet with viscous dissipation with and without porous medium. Nayak et al. [14] discussed the unsteady radiative MHD free convective flow and mass transfer of a viscoelastic fluid past an inclined porous plate. Cortell [15] has worked on viscous flow and heat transfer over a nonlinearly stretching sheet. Effect of viscous dissipation and radiation on the thermal boundary layer over a nonlinearly stretching sheet was also studied by Cortell [16].

Singh [17] and Chen [18] contributed recently to this field of study. All their works are related to viscoelastic fluid model in the presence of magnetic field. They considered either an oscillatory stretching

surface or surface with a linearly varying velocity. They have used hyper-geometric function i.e., Kummer's function. All these works reported above considered either radiation effect/viscous dissipation or both. The novelty of the present study is starred due to the following three aspects.

1. Inclusion of porous media is justified since the flow and heat transport processes occur by using insulating material (porous matrix) which greatly prevents heat loss and accelerates the process of cooling/heating as the case may be serving as a heat exchanger.
2. Consideration of mass diffusion as the flow of industrial fluids is subjected to more than one fluid either generated/provided externally.
3. Inclusion of chemical reaction term in the mass transport equation which is vital since the fluids may be chemically reactive.

Second grade or Walters' B models are considered in the present study. This is because this two models provide relative response to flow and heat transfer rate. Moreover, elastic property of Walters' B flow model reduces the flow instabilities which are mainly driven by the fluid normal stresses or by the nature of boundary conditions.

The present study is a generalized approach by which we can discuss the results of Chen [18] as a special case, without considering mass diffusion and porous medium. Moreover, it is intended to bring out the effects of the emerging parameters on the heat and mass transport phenomena. The confluent hypergeometric function i.e. Kummer's function has been used to solve the heat and mass transport equations after using similarity transformation which reduces the governing partial differential equations into to ordinary differential equations.

2 Formulation of the problem

Consider a steady two-dimensional boundary-layer flow of an electrically conducting, viscoelastic fluid past a stretching sheet embedded in a porous medium, the flow being confined to $y > 0$. Two equal and opposite forces are applied along x-axis so that the surface is stretched, keeping the origin fixed. Assuming that a uniform magnetic field of strength B_0 is applied along y-axis that generates magnetic effect in the x-direction. Under the usual boundary layer assumptions, the equations of continuity, momentum, energy and species concentration for the flow of viscoelastic fluid are:

$$\frac{\partial u}{\partial x} + \frac{\partial v}{\partial y} = 0 \tag{1}$$

$$u \frac{\partial u}{\partial x} + v \frac{\partial u}{\partial y} = v \frac{\partial^2 u}{\partial y^2} + \frac{k_0}{\rho} \left(\frac{\partial}{\partial x} \left(u \frac{\partial^2 u}{\partial y^2} \right) + v \frac{\partial^3 u}{\partial y^3} - \frac{\partial u}{\partial y} \frac{\partial^2 u}{\partial x \partial y} \right) - \frac{\sigma B_0^2 u}{\rho} - \frac{vu}{K_p'} \tag{2}$$

$$\rho C_p \left(u \frac{\partial T}{\partial x} + v \frac{\partial T}{\partial y} \right) = k \frac{\partial^2 T}{\partial y^2} + \mu \left(\frac{\partial u}{\partial y} \right)^2 + k_0 \left(\frac{\partial u}{\partial y} \frac{\partial}{\partial y} \left(u \frac{\partial u}{\partial x} + v \frac{\partial u}{\partial y} \right) \right) + \sigma B_0^2 u^2 - \frac{\partial q_r}{\partial y} + q(T - T_\infty) \tag{3}$$

$$u \frac{\partial C}{\partial x} + v \frac{\partial C}{\partial y} = D \frac{\partial^2 C}{\partial y^2} - K_c'(C - C_\infty) \tag{4}$$

Rosseland's approximation for thermal radiation gives $q_r = -\frac{4\sigma^*}{3k_1} \frac{\partial(T^4)}{\partial y}$. It is assumed that the temperature variation within the flow is such that T^4 may be expanded in a Taylor series. Expanding T^4 about T_∞ and neglecting the higher order terms, we have

$$T^4 = 4T_\infty^3 T - 3T_\infty^4 \quad \text{and} \quad \frac{\partial q_r}{\partial y} = -\frac{16\sigma^* T_\infty^3}{3k_1 \rho C_p} \frac{\partial^2 T}{\partial y^2}.$$

Substituting the above value of $\frac{\partial q_r}{\partial y}$ in Eq. (3), we get

$$u \frac{\partial T}{\partial x} + v \frac{\partial T}{\partial y} = \alpha \frac{\partial^2 T}{\partial y^2} + \frac{\mu}{\rho C_p} \left(\frac{\partial u}{\partial y} \right)^2 + \frac{k_0}{\rho C_p} \left(\frac{\partial u}{\partial y} \frac{\partial}{\partial y} \left(u \frac{\partial u}{\partial x} + v \frac{\partial u}{\partial y} \right) \right) + \frac{16\sigma^* T_\infty^3}{3k_1 \rho C_p} \frac{\partial^2 T}{\partial y^2} + \frac{q}{\rho C_p} (T - T_\infty) + \frac{\sigma B_0^2}{\rho C_p} u^2 \tag{5}$$

The boundary conditions are:

$$
\left.
\begin{aligned}
&u = u_w = Ex, \quad v = v_w, \quad T = T_w(x) = T_\infty + A\left(\frac{x}{L}\right)^2 (PST\ case), \\
&h_w(x) = -k\left(\frac{\partial T}{\partial y}\right) = B\left(\frac{x}{L}\right)^2 (PHF\ case), \\
&C = C_w(x) = C_\infty + E_0\left(\frac{x}{L}\right)^2, \, m_w = -D\left(\frac{\partial C}{\partial y}\right) = E_1 x^2, \quad\quad at\ y \to 0 \\
&u = 0, \frac{\partial u}{\partial y} = 0, T \to T_\infty, C \to C_\infty \quad\quad\quad\quad\quad as\ y \to \infty
\end{aligned}
\right\}
\tag{6}
$$

3 Solution of the flow field

Equations (1) and (2) admit self–similar solutions of the form

$$
f = \frac{\psi}{\upsilon\sqrt{\mathrm{Re}_x}}, \quad \eta = \frac{y}{x}\sqrt{\mathrm{Re}_x}
\tag{7}
$$

where f is the dimensionless stream function and η is the similarity variable and $\mathrm{Re}_x = u_w x/\upsilon$ is the local Reynolds number, $\psi(x,y)$ is the stream function satisfying the continuity Eq. (1).

Substituting Eqs. (7) in (2), we get

$$
\begin{aligned}
&f''' + ff'' - (f')^2 + R_c\Big\{2f'f''' - (f'')^2 - ff^{iv}\Big\} \\
&- \left(M_n + \frac{1}{K_p}\right)f' = 0,
\end{aligned}
\tag{8}
$$

where $R_c = k_0 E/\mu$ is the viscoelastic parameter, $M_n = \sigma B_0^2/\rho E$ is the magnetic parameter and $K_p = \frac{EK_p'}{\nu}$ is the non-dimensional permeability parameter.

The corresponding boundary conditions are:

$$
f(0) = f_w, f'(0) = 1, f'(\infty) = 0, f''(\infty) = 0.
\tag{9}
$$

where $f_w = \frac{-v_w\sqrt{\mathrm{Re}_x}}{u_w}$ is the suction/injection parameter, $f_w > 0$ and $f_w < 0$ represent suction and injection respectively.

The exact solution of Eq. (8) with boundary conditions expressed in Eq. (9) following Chakrabati and Gupta [19] is in the form

$$
f(\eta) = \frac{1 - e^{-r\eta}}{r} + f_w,
\tag{10}
$$

where r is a real positive root of the cubic algebraic equation

$$
R_c f_w r^3 + (R_c + 1)r^2 - f_w r - \left(1 + M_n + \frac{1}{K_p}\right) = 0
\tag{11}
$$

The velocity profile can be obtained from the Eq. (10) as

$$
f'(\eta) = e^{-r\eta}
\tag{12}
$$

The shear stress at the wall is defined as

$$
\tau_w = \mu\left(\frac{\partial u}{\partial y}\right)_{y=0} = \mu Ex\sqrt{E/\nu}.f''(0)
\tag{13}
$$

The non dimensional form of skin friction coefficient at the wall is

$$
C_f R_{e_x}^{1/2} = -f''(0) = r
\tag{14}
$$

4 Heat transfer analysis

4.1 Case I: Prescribed surface temperature (PST)

In prescribed surface temperature case, introducing non-dimensional quantities $\theta(\eta) = \frac{T - T_\infty}{T_w - T_\infty}$, $P_r = \nu/\alpha$, $E_c = \frac{E^2 l^2}{A C_p}$, $R_c = \frac{Ek_0}{\mu}$, $Q = \frac{q}{E\rho C_p}$, $R = \frac{16\sigma^* T_\infty^3}{3k_1 k}$ and using Eq. (6), the Eq. (5) becomes

$$
\begin{aligned}
&(1 + R)\theta'' + P_r f\theta' + P_r(Q - 2f')\theta \\
&= -E_c P_r\Big((f'')^2 + R_c(f'f'' - ff''') \\
&\quad + \left(M_n + \frac{1}{K_p}\right)(f')^2\Big)
\end{aligned}
\tag{15}
$$

with the boundary conditions

$$\theta(0) = 1, \theta(\infty) = 0 \qquad (16)$$

Introducing the variable $\xi = -\frac{P_r e^{-r\eta}}{(1+R)r^2}$ the Eq. (15) transformed to

$$\xi \frac{d^2\theta}{d\xi^2} + \left(1 - \frac{P_r S}{(1+R)r^2} - \xi\right)\frac{d\theta}{d\xi}$$
$$+ \left(\frac{P_r Q}{(1+R)r^2\xi} + 2\right)\theta$$
$$= -\frac{E_c(1+R)r^4}{P_r}\left[1 + R_c S + \frac{1}{r^2}\left(M_n + \frac{1}{K_p}\right)\right]\xi \qquad (17)$$

with the boundary conditions

$$\theta\left(\xi = -\frac{P_r}{(1+R)r^2}\right) = 1, \quad \theta(\xi = 0) = 0 \qquad (18)$$

where $S = 1 + r f_w$. Using confluent hypergeometric function of first kind (Kummer's function) we get,

$$\theta(\xi) = \left[1 + \frac{E_c P_r\left(1 + R_c S + \frac{1}{r^2}\left(M_n + \frac{1}{K_p}\right)\right)}{(1+R)\{4 - (2S - Q)P_r^*\}}\right]$$
$$\left(\frac{\xi}{-P_r^*}\right)^a \frac{M(a-2, b+1, \xi)}{M(a-2, b+1, -P_r^*)}$$
$$- \frac{E_c P_r\left(1 + R_c S + \frac{1}{r^2}\left(M_n + \frac{1}{K_p}\right)\right)}{(1+R)\{4 - (2S - Q)P_r^*\}}\left(\frac{\xi}{P_r^*}\right)^2 \qquad (19)$$

where

$$a = \frac{P_r^* S + \sqrt{(P_r^* S)^2 - 4P_r^* Q}}{2},$$
$$b = \sqrt{(P_r^* S)^2 - 4P_r^* Q}, P_r^* = \frac{P_r}{(1+R)r^2}, S = 1 + r f_w$$

and $M(\alpha_1, \alpha_2; x)$ denotes the Kummer's function and is given by

$$M(\alpha_1, \alpha_2; x) = \sum_{n=0}^{\infty}\frac{(\alpha_1)_n}{(\alpha_2)_n}\frac{x^n}{n!}, \quad \alpha_2 \neq 0, -1, -2\ldots \qquad (20)$$

where $(\alpha)_n$ denoting the Pochhammer symbol defined in terms of the gamma function as

$$(\alpha)_n = \alpha(\alpha+1)(\alpha+2)\cdots(\alpha+n-1) = \frac{\Gamma(\alpha+n)}{\Gamma(\alpha)} \qquad (21)$$

The temperature profile in terms of η can be written as

$$\theta(\eta) = \left[1 + \frac{E_c P_r\left\{1 + R_c S + \frac{1}{r^2}\left(M_n + \frac{1}{K_p}\right)\right\}}{(1+R)\{4 - (2S - Q)P_r^*\}}\right]$$
$$e^{-ar\eta}\frac{M(a-2, b+1, -P_r^* e^{-r\eta})}{M(a-2, b+1, -P_r^*)}$$
$$- \frac{E_c P_r\left\{1 + R_c S + \frac{1}{r^2}\left(M_n + \frac{1}{K_p}\right)\right\}}{(1+R)\{4 - (2S - Q)P_r^*\}}e^{-2r\eta} \qquad (22)$$

The dimensionless wall temperature gradient is given by

$$\theta\prime(0) = r\left[1 + \frac{E_c P_r\left\{1 + R_c S + \frac{1}{r^2}\left(M_n + \frac{1}{K_p}\right)\right\}}{(1+R)\{4 - (2S - Q)P_r^*\}}\right]$$
$$\times \left[P_r^*\left(\frac{a-2}{b+1}\right)\frac{M(a-1, b+2, -P_r^*)}{M(a-2, b+1, -P_r^*)} - a\right]$$
$$+ 2r\left[\frac{E_c P_r\left\{1 + R_c S + \frac{1}{r^2}\left(M_n + \frac{1}{K_p}\right)\right\}}{(1+R)\{4 - (2S - Q)P_r^*\}}\right] \qquad (23)$$

The local Nusselt number for PST case is

$$N_{u_x}\text{Re}_x^{-1/2} = -\theta'(0) \qquad (24)$$

4.2 Case II: Prescribed heat flux (PHF)

In prescribed heat flux case, introducing the similarity variable $T - T_\infty = \frac{Bx^2}{kL^2}\sqrt{\frac{v}{E}}\,\psi(\eta)$ and using Eqs. (6), (5) becomes

$$(1+R)\psi'' + P_r f\psi' + P_r(Q - 2f')\psi$$
$$= -E_c P_r\left[(f'')^2 + R_c f''(f'f'' - ff''')\right.$$
$$\left. + \left(M_n + \frac{1}{K_p}\right)(f')^2\right] \qquad (25)$$

with the boundary conditions

$$\psi(0) = -1, \quad \psi(\infty) = 0 \qquad (26)$$

where $E_c = \frac{E^2 L^2 k \sqrt{E/v}}{B C_p}$ is the Eckert number and the other parameters are as defined in the PST case.

Substituting $\xi = -\frac{P_r e^{-r\eta}}{(1+R)r^2}$ in Eqs. (25) and (26) we get respectively

$$\xi \frac{d^2\psi}{d\xi^2} + \left(1 - \frac{P_r S}{(1+R)r^2} - \xi\right)\frac{d\psi}{d\xi} + \left(\frac{P_r Q}{(1+R)r^2\xi} + 2\right)\psi$$
$$= -\frac{E_c(1+R)r^4}{P_r}\left[1 + R_c S + \frac{1}{r^2}\left(M_n + \frac{1}{K_p}\right)\right]\xi \tag{27}$$

$$\psi(\xi = 0) = 0,$$
$$\psi'\left(\xi = -\frac{P_r}{(1+R)r^2}\right) = -\frac{(1+R)r}{P_r} \tag{28}$$

The exact solution of Eq. (27) subject to the boundary conditions expressed in Eq. (28) can be written in terms of confluent hypergeometric function in terms of similarity variable η and is given by

$$\psi(\eta) = \frac{\left[\frac{1}{r} + 2\left[\frac{E_c P_r\left\{1 + R_c S + \frac{1}{r^2}\left(M_n + \frac{1}{K_p}\right)\right\}}{(1+R)\{4 - (2S-Q)P_r^*\}}\right]\right] \cdot e^{-ar\eta} \cdot M\left(a - 2, b + 1; -P_r^* e^{-r\eta}\right)}{aM(a - 2, b + 1; -P_r^*) - P_r^*\left(\frac{a-2}{b+1}\right)M(a - 1, b + 2; -P_r^*)}$$
$$- \left[\frac{E_c P_r\left\{1 + R_c S + \frac{1}{r^2}\left(M_n + \frac{1}{K_p}\right)\right\}}{(1+R)\{4 - (2S-Q)P_r^*\}}\right] \cdot e^{-2r\eta} \tag{29}$$

The dimensionless wall temperature can be expressed as

$$\psi(\eta) = \frac{\frac{1}{r} + 2\left[\frac{E_c P_r\left\{1 + R_c S + \frac{1}{r^2}\left(M_n + \frac{1}{K_p}\right)\right\}}{(1+R)\{4 - (2S-Q)P_r^*\}}\right] \cdot M(a - 2, b + 1; -P_r^*)}{a \cdot M(a - 2, b + 1; -P_r^*) - P_r^*\left(\frac{a-2}{b+1}\right)M(a - 2, b + 2; -P_r^*)} - \left[\frac{E_c P_r\left\{1 + R_c S + \frac{1}{r^2}\left(M_n + \frac{1}{K_p}\right)\right\}}{(1+R)\{4 - (2S-Q)P_r^*\}}\right] \tag{30}$$

The local Nusselt number for the PHF case can be written as

$$N_{u_x} R_{e_x}^{-1/2} = \frac{1}{\psi(0)} \tag{31}$$

5 Mass transfer analysis

Introducing the similarity variable $C - C_\infty = \frac{E_1 x^2}{D}\sqrt{\frac{v}{E}}\phi(\eta)$ and using Eqs. (6) in (4),

$$\phi'' + S_c f \phi' - S_c f' \phi - S_c K_c \phi = 0 \tag{32}$$

with the boundary conditions

$$\begin{aligned} \phi' &= -1 \quad \text{at} \quad \eta = 0 \\ \phi &\to 0 \quad \text{at} \quad \eta \to \infty \end{aligned} \tag{33}$$

Again introducing a new variable $\xi = -\frac{S_c}{r^2}e^{-r\eta}$, the Eq. (32) becomes
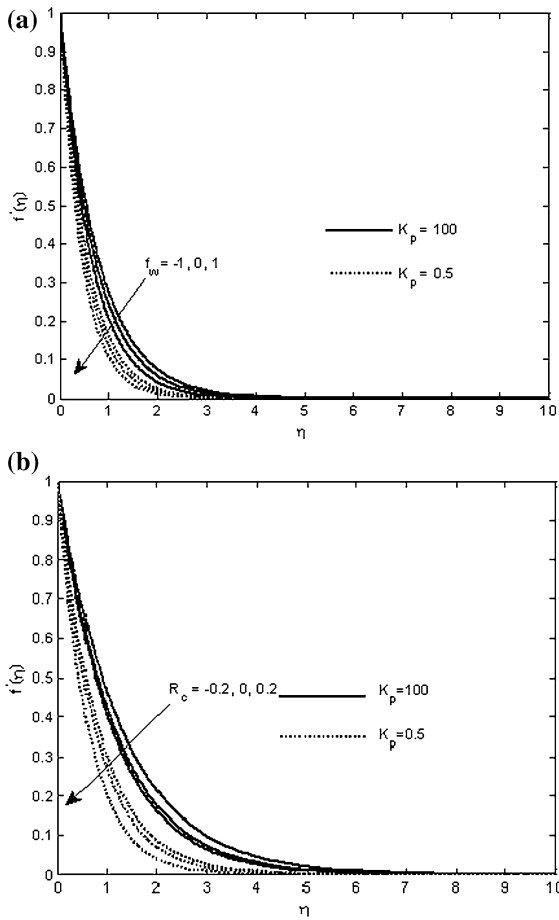
Fig. 1 a Velocity profiles (second grade fluid) for $M_n = 0.5$, $R_c = 1$. **b** Velocity profiles for $M_n = 1$, $f_w = 0$

$$\xi \frac{d^2\phi}{d\xi^2} + \left[\left(1 - \frac{S_c}{r^2}\left(r^2 - M_n - \frac{1}{K_p}\right)\right) - \xi\right]\frac{d\phi}{d\xi} + \left(2 - \frac{K_c}{r^2\xi}\right)\phi = 0 \tag{34}$$

The corresponding boundary conditions are

$$\phi(\xi = 0) = 0, \quad \phi'\left(\xi = -\frac{S_c}{r^2}\right) = -\frac{r}{S_c} \tag{35}$$

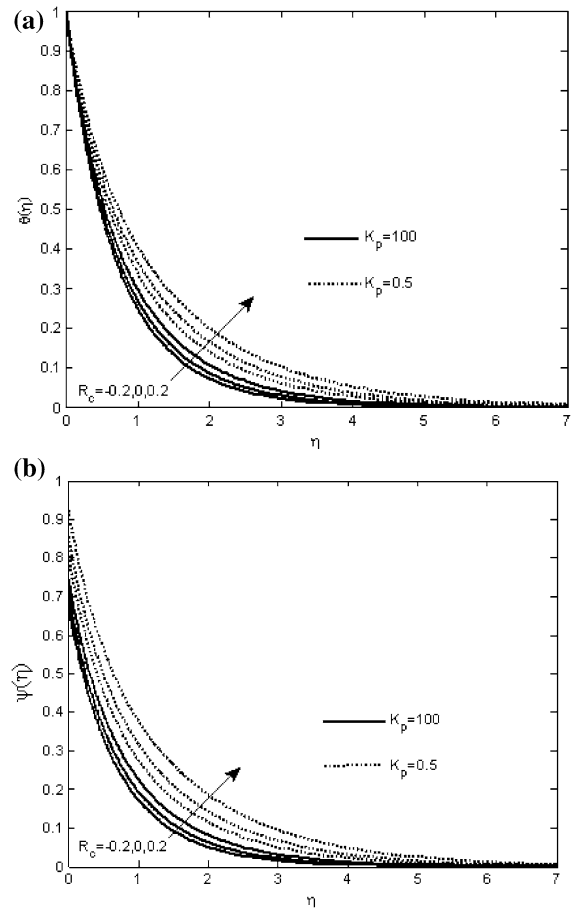The exact solution of Eq. (34) subject to the boundary condition expressed in Eq. (35) is given by

Fig. 2 a Temperature profiles for $P_r = 3, M_n = 1, E_c = 0.1, R = 1, Q = 0, f_w = 0$ (PST case). **b** Temperature profiles for $P_r = 3, M_n = 1, E_c = 0.1, R = 1, Q = 0, f_w = 0$ (PHF case)

where $S_1 = \frac{S_c}{r^2}\left[r^2 - \left(M^2 + \frac{1}{K_p}\right)\right]$ and $S_2 = \sqrt{S_1^2 + \frac{4K_c}{r^2}}$. The dimensionless wall concentration gradient is given by

$$\phi(\eta) = \frac{e^{-\left(\frac{S_1+S_2}{2}\right) r\eta} M\left(\frac{S_1+S_2-4}{2}, 1 + S_1; -\frac{S_c}{r^2} \cdot e^{-r\eta}\right)}{\frac{r(S_1+S_2)}{2} \cdot M\left(\frac{S_1+S_2-4}{2}, 1 + S_1, -\frac{S_c}{r^2}\right) - \frac{S_c}{r}\left[\left(\frac{S_1+S_2-2}{2(1+S_1)}\right) M\left(\frac{S_1+S_2-2}{2}, 2 + S_1, -\frac{S_c}{r^2}\right)\right]} \tag{36}$$

$$\phi'(0) = \frac{-r^{\left(\frac{S_1+S_2}{2}\right)} M\left(\frac{S_1+S_2-4}{2}, 1+S_1; -\frac{S_c}{r^2}.e^{-r\eta}\right) + M\left(\frac{S_1+S_2-2}{2}, 2+S_1; -\frac{S_c}{r^2}.e^{-r\eta}\right)}{\frac{r(S_1+S_2)}{2}.M\left(\frac{S_1+S_2-4}{2}, 1+S_1, -\frac{S_c}{r^2}\right) - \frac{S_c}{r}\left[\left(\frac{S_1+S_2-2}{2(1+S_1)}\right) M\left(\frac{S_1+S_2-2}{2}, 2+S_1, -\frac{S_c}{r^2}\right)\right]} \tag{37}$$

The local Sherwood number can be expressed as

$$S_{h_x} \mathrm{Re}_x^{-1/2} = -\phi'(0) \tag{38}$$

6 Results and discussion

In the course of discussion the following aspects are highlighted.

1. Effect of permeability of the medium on flow characteristics.

2. Effect of diffusion species as well as first order chemical reaction

3. Relative response of two viscoelastic models to velocity and temperature distribution in the presence of uniform porous matrix.

4. Presenting the generality of the present study by discussing the previous result as particular case.

It is important to note that $R_c > 0$, $R_c < 0$ and $R_c = 0$ represent second grade, Walters $B\prime$ and viscous fluids respectively.

Fig. 3 **a** Temperature profiles for $P_r = 1, M_n = 1, R_c = 1, R = 0, Q = 0, f_w = 0$ (PST case). **b** Temperature profiles for $P_r = 3, M_n = 1, E_c = 0.1, R_c = 1, R = 0, Q = 0, f_w = 0$ (PHF case)

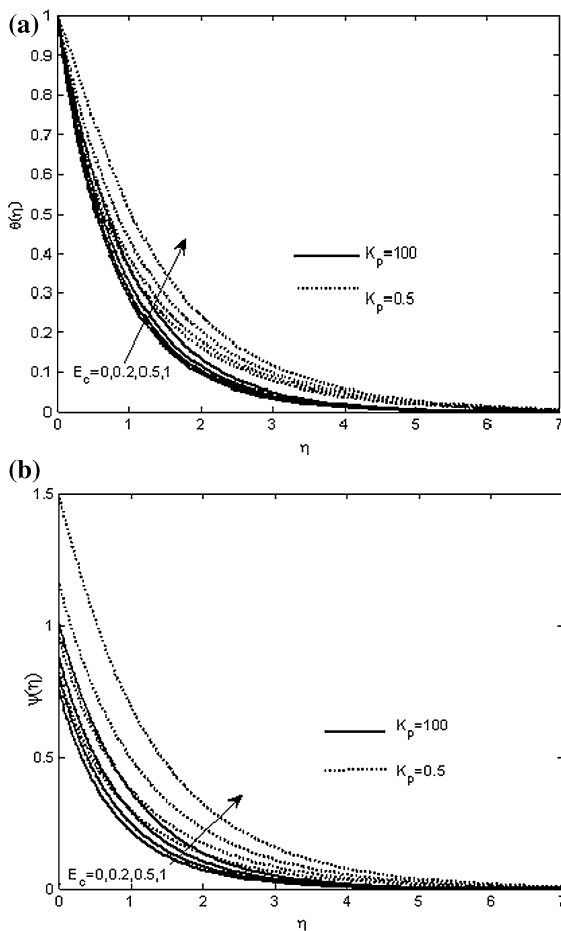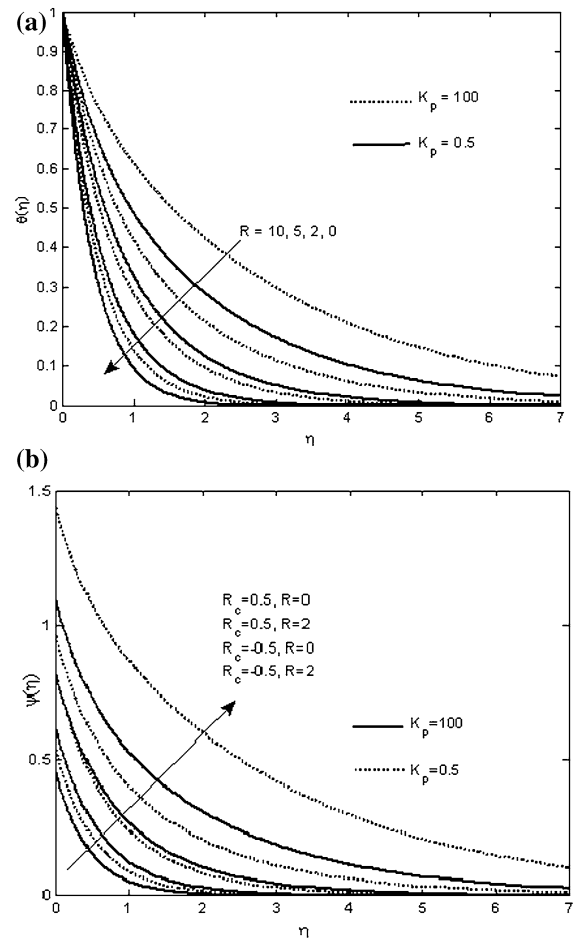Fig. 4 **a** Temperature profiles for $P_r = 3, M_n = 1, E_c = 0.1, R_c = 0.5, Q = 0, f_w = 0$ (PST case). **b** Temperature profiles for $P_r = 3, M_n = 1, E_c = 0.1, Q = 0, f_w = 0$ (PHF case)
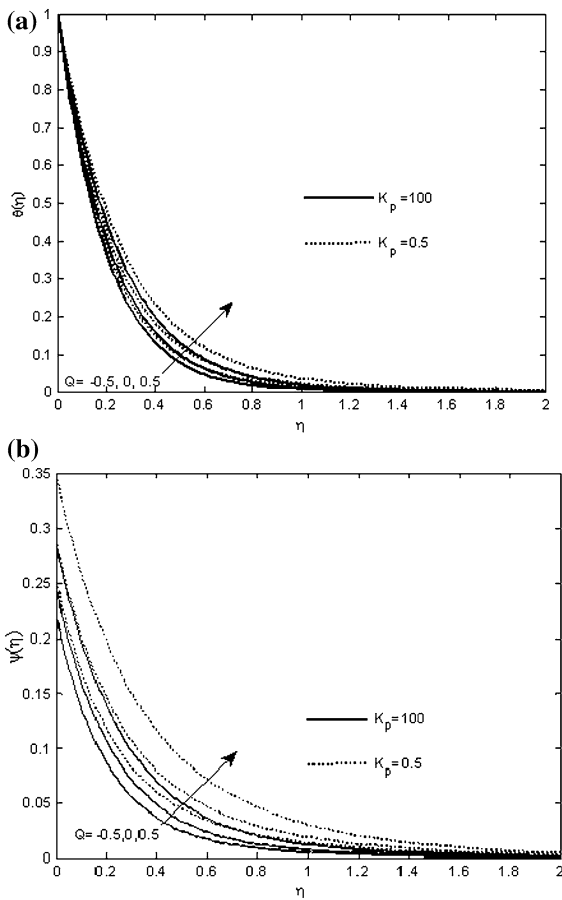
Fig. 5 **a** Temperature profiles for $P_r = 3, M_n = 1, E_c = 0.1, R_c = 0.5, R = 0, f_w = 0.5$ (PST case). **b** Temperature profiles for $P_r = 3, M_n = 1, E_c = 0.1, R_c = 0.5, R = 0, f_w = 0.5$ (PHF case)

Fig. 6 Concentration profiles

Table 1 Skin friction coefficients

M_n	K_p	R_c	$\tau(f_w = 0)$	$\tau(f_w = 1)$
1	100	−0.5	−2.00499	1.002852
1	0.5	−0.5	−2.82843	1.445428
0.5	100	−0.5	−1.73781	0.847162
0.5	0.5	−0.5	−2.64575	1.351683
1	100	0.5	−1.15758	1.004
1	0.5	0.5	−1.63299	2
0.5	100	0.5	−1.00333	0.802458
0.5	0.5	0.5	−1.52753	1.65662
1	100	1.0	−1.0025	1.005013
1	0.5	1.0	−1.41421	−1.26953
0.5	100	1.0	−0.86891	0.774667
0.5	0.5	1.0	−1.32288	−1.21124

Figure 1a shows the velocity distribution of second grade fluid for suction ($f_w > 0$), injection ($f_w < 0$) and impermeable plate ($f_w = 0$) in the presence ($K_p = 0.5$) and absence ($K_p = 100$) of porous matrix. The profiles $K_p = 100$, $M_n = 0.5$, $R_c = 1$ coincides with Fig. 1b of Chen [18] and hence our result finds a good agreement. The porous medium ($K_p = 0.5$) reduces the primary velocity at all points due to resistive force offered by the porous medium which results in thinning of boundary layer. Further, it is interesting to note that the suction at the plate reduces the velocity. Thus, it is concluded that combined effect of suction and porous matrix favorable to thinning of boundary layer which favors the stability of the flow.

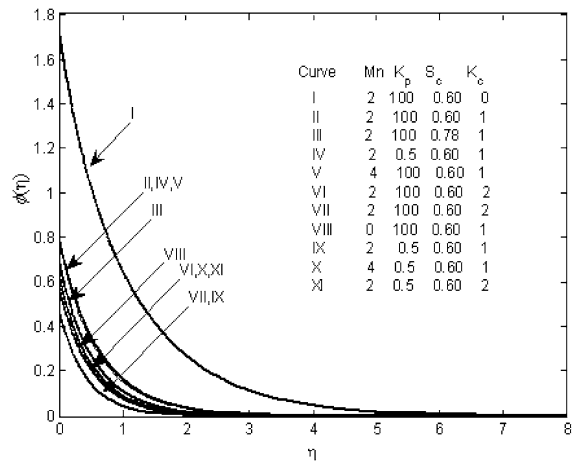Figure 1b exhibits the velocity profiles for Walters B' ($R_c = -0.2$), viscous ($R_c = 0$) and second grade flow ($R_c = 0.2$). It is observed that velocity attains low value in case of visco-elasticity (Walters B' model), in the presence of porous medium. Viscoelastic flows are prone to instabilities due to non-linearity in the constitutive equations. Instability are mainly driven by the fluid normal stresses (elasticity) or by the nature of the boundary conditions. Therefore, elastic property of Walters flow model in conjunction with the permeability of the porous medium reduces the boundary layer thickness and hence reduces the instability.

Figures 2a, b display the temperature distribution in case of PST and PHF cases respectively without suction/injection. The effects of the permeability of the medium and elasticity of the fluid subject to

Table 2 Comparison of Nusselt numbers to Liu [20] for a second-grade fluid for $R_c = 1.0$, $E_c = 0.2$, $R = 0$ and $f_w = 0$

M_n	K_p	Q	P_r	PST case		PHF case	
				Liu [20]	Present case	Liu [20]	Present case
0.0	100	−0.1	1	1.37488	1.372608	0.742096	0.7435
	100	−0.1	10	4.59962	4.591724	0.276367	0.277832
	0.5	−0.1	1		1.032946		0.975079
	0.5	−0.1	10		3.249158		0.536112
	100	0	1	1.337265	1.331574	0.764213	0.765383
	100	0	10	4.48696	4.478859	0.284146	0.28568
	0.5	0	1		0.974733		1.019901
	0.5	0	10		3.103711		0.55611
	100	0.1	1	1.29111	1.288637	0.788006	0.789645
	100	0.1	10	4.37115	4.362827	0.292579	0.294189
	0.5	0.1	1		0.906795		1.077075
	0.5	0.1	10		2.952014		0.578134
1.0	100	−0.1	1	1.18298	1.181325	0.876313	0.868455
	100	−0.1	10	3.87868	3.87202	0.412923	0.414209
	0.5	−0.1	1		0.906259		1.073528
	0.5	−0.1	10		2.676623		0.65084
	100	0	1	1.13333	1.131589	0.9	0.901256
	100	0	10	3.74805	3.741224	0.427117	0.428464
	0.5	0	1		0.839487		1.132026
	0.5	0	10		2.518129		0.67632
	100	0.1	1	1.0792	1.077335	0.938308	0.939725
	100	0.1	10	3.61261	3.605617	0.442665	0.444078
	0.5	0.1	1		0.75274		1.216857
	0.5	0.1	10		2.352002		0.704501

present study on temperature distribution are opposite to that of viscous dissipation that is the temperature increases at all points and this is further contributed by Walters B' model. Both the cases of PST and PHF display the same effect.

Figures 3a, b illustrate the effects of Eckert number in case of second grade fluid in the absence of suction/injection and thermal radiation in both PST and PHF cases. The energy dissipation of the flow configuration is measured by Eckert number. It is seen that an increase in E_c increases the temperature and hence increases the thermal boundary layer thickness. This leads to reduction of the rate of heat transfer from the plate surface. This reduction is further decreased due to presence of porous medium. Therefore, the presence of porous medium acts as an insulator to the plate surface. This result is in good agreement with the result of Chen [18].

Figure 4a, b delineate the effect of radiation parameter in case of second grade fluid. It is observed that an increase in thermal radiation parameter (R) increases the temperature of the fluid layer and the processes get accelerated due to the presence of the porous matrix. The increase in temperature with an increase in radiation parameter causes a reduction in temperature gradient of the wall in PST case. Thus, it is concluded that thermal radiation is to reduce in order to make the cooling process faster.

Figure 5a, b exhibit the effect of the internal heat generation/absorption parameter (Q) on the temperature distribution $\theta(\eta)$ (PST) and $\psi(\eta)$ (PHF) in case of second grade fluid. This shows that an increase in heat source strength ($Q > 0$) increases the temperature. This is due to generation of the heat in thermal boundary layer which causes the temperature to rise. In similar manner the heat sink causes the temperature

Table 3 Comparison of Nusselt numbers to Datti et al. [21] for Walters' liquid B'

P_r	R_c	M_n	K_p	Q	R	PST case		PHF case	
						Datti et al. [21]	Present case	Datti et al. [21]	Present case
1	0	0	100	0	0	1.3333	1.331932		0.750789
1	0	0	100	−0.1	0		1.377796	0.7251	0.725797
1	0	0	0.5	0	0		1.126898		0.887391
1	0	0	0.5	−0.1	0		1.199394		0.833755
1	0	1	100	0	0	1.2158	1.214771		0.823201
1	0	1	100	−0.1	0		1.274028	0.7843	0.784912
1	0	1	0.5	0	0		1.055361		0.947543
1	0	1	0.5	−0.1	0		1.140395		0.876889
1	−0.1	0.1	100	−0.1	0	1.3521	1.350924	0.7395	0.740234
1	−0.1	0.1	100	0	0	1.3035	1.302129	0.7671	0.767973
1	−0.1	0.1	100	0.1	0	1.2496	1.247923	0.8002	0.801332
1	−0.1	0.1	0.5	−0.1	0		1.17154		0.853577
1	−0.1	0.1	0.5	0	0		1.093343		0.914626
1	−0.1	0.1	0.5	0.1	0		0.971376		1.026597
1	−0.1	0.1	100	−0.1	1	0.8812	0.874755	1.1348	1.143177
1	−0.1	0.1	0.5	−0.1	1		0.722385		1.384303
2	−0.1	0.1	100	−0.1	0	2.021	2.027636	0.4928	0.493185
2	−0.1	0.1	0.5	−0.1	0		1.17154		0.853577
3	−0.1	0.1	100	−0.1	0	2.5326	2.546397	0.3926	0.392712
3	−0.1	0.1	0.5	−0.1	0		2.357059		0.424257

Table 4 Sherwood number

M_n	K_p	S_c	K_c	S_h
3	100	0.6	0	1.331674
3	100	0.6	1	−1.90499
3	0.5	0.6	1	−2.35153
4	100	0.6	1	−2.14054
3	100	0.78	1	−1.90499
3	100	0.6	2	−1.93499

absorption resulting in decrease in temperature. The result holds good for both PST and PHF. The role of porous matrix is to accelerate/decelerate the process in case of source/sink respectively.

Figure 6 exhibits the concentration profiles for various values of the parameters characterizing the concentration distribution. It is observed that chemical reaction parameter reduces the concentration distribution at all points irrespective of the presence or absence of porous matrix. From the curves V and X it is seen that the presence of porous matrix enhances the concentration level at all points of the flow domain in the presence of chemical reaction. Now, it is further seen that the effect of magnetic field is to increase the concentration (Curve II, $M = 2$, Curve VIII, $M = 0$) but further increase in M has no significant effect on concentration field in the absence of porous matrix whereas in the presence of porous matrix (Curves IV and IX) an increase in magnetic field reduces the concentration level. Moreover, heavier species (high value of S_c) contributes to the reduction in the level of concentration in the absence of porous matrix (Curve II and III).

From Table 1 it is noticed that an increasing magnetic parameter enhances the skin friction and it is further increased due to the presence of porous matrix. However, elasticity effect increases the skin friction. Thus, it is concluded that higher value of elastic elements is favorable in enhancing the skin friction in both impermeable ($f_w = 0$) and permeable ($f_w \neq 0$) surfaces.

Tables 2 and 3 show the comparison of temperature gradients for second grade and second order fluids in PST and PHF cases respectively. On comparison it is

observed that the results accomplished by Liu [20] and Datti et al. [21] well agree with the present study. From Table 2, it is seen that the absence of porous matrix and magnetic parameter with higher Prandtl value cause the Nusselt number to increase irrespective of source/sink in PST whereas, the reverse effect is attained in PHF. It is also seen that in the presence of porous matrix, the reverse trend appears in both PST and PHF. It is interesting to mention that in the presence of magnetic parameter with higher Prandtl value, the Nusselt number decreases in PST and increases in PHF in presence/absence of porous matrix and source/sink. Thus, it is concluded that for second grade fluid, the characteristics of Nusselt number are achieved in the permeable surface ($f_w = 0$) without thermal radiation ($R = 0$). From Table 3 it is observed that absence of porous matrix with high P_r enhances the Nusselt number in PST and reduces in PHF and the reverse effect is attained in the presence of the porous matrix but increasing value of magnetic parameter, presence/absence of source/sink parameter and thermal radiation parameter lead to the reverse effects in both PST and PHF. Therefore, the rate of heat transfer is influenced by the presence of porous matrix, magnetic parameter and thermal radiation parameter causes instability in the rate of heat transfer phenomena.

Table 4 enlists the numerical values of the rate of mass transfer at the plate. It is interesting to observe that absence of chemical reaction contributes to positive value whereas presence of it gives rise to negative values. It is noticed that an increase in magnetic parameter (M_n), porosity parameter (K_p) and Schmidt parameter (S_c) (that is for heavier species) enhances the Sherwood number whereas increase in chemical reaction parameter decreases the Sherwood number.

7 Conclusion

1. Porous matrix acting as an insulator to the vertical surface prevents energy loss due to free convection which in turn enhances the velocity.
2. Presence of porous matrix and elasticity of the fluid overcomes the resistive force of magnetic field and hence the velocity increases due to the presence of both.
3. Presence of elasticity also leads to increase the temperature at all points irrespective of presence/absence of porous matrix.
4. The slow rate of thermal diffusion in presence of magnetic field and porous matrix causes thinning of thermal boundary layer thickness.
5. The variation in temperature is more sensitive on account of heat flux.
6. Presence of chemical reaction as well as porous matrix with moderate values of magnetic parameter in case of heavier species reduces the concentration level.
7. Higher value of magnetic field in conjunction with porous matrix reduce the concentration level.
8. Presence of elastic element favors in reducing the skin friction in both permeable and impermeable surfaces.
9. Presence of magnetic parameter causes to decrease the Nusselt number in PST case and increase the same in PHF case
10. Presence of porous matrix and magnetic parameter influences the rate of heat transfer.
11. Porous matrix enhances the rate of mass transfer whereas increase in chemical reaction has no impact on the absence of porous matrix.

References

1. Sakiadis BC (1961) Boundary layer behavior on continuous solid surface I. Boundary-layer equations for two dimensional and axisymmetric flow. AIChE J 7(1):26–28
2. Crane LJ (1970) Flow past a stretching plane. Z Angew Math Phys (ZAMP) 21(4):645–647
3. Khan SK, Sanjayanand E (2005) Viscoelastic boundary layer flow and heat transfer over an exponential stretching sheet. Int J Heat Mass Transf 48:1534–1542
4. Kar M, Sahoo SN, Rath PK, Rath GC (2014) Heat and mass transfer effects on a dissipative and radiative viscoelastic MHD flow over a stretching porous sheet. Arab J Sci Eng 39(5):3393–3401
5. Nayak MK, Dash GC, Singh LP (2014) Effect of chemical reaction on MHD flow of a visco-elastic fluid through porous medium. J Appl Anal Comput 4(4):367–381
6. Hayat T, Asad S, Mustafa M, Alsaedi A (2015) MHD stagnation-point flow of Jeffrey fluid over a convectively heated stretching sheet. Comput Fluids 108:179–185
7. Bataller RC (2007) Viscoelastic fluid flow and heat transfer over a stretching sheet under the effects of a non-uniform heat source, viscous dissipation and thermal radiation. Int J Heat Mass Transf 50:3152–3162

8. Hayat T, Awais M, Safdar A, Hendi AA (2012) Unsteady three dimensional flow of couple stress fluid over a stretching surface with chemical reaction. Non-Linear Anal Model Control 17:47–59

9. Gireesha BJ, Chamkha AJ, Manjunatha S, Bagewadi CS (2013) Boundary-layer flow and heat transfer of a dusty fluid flow over a stretching sheet with non-uniform heat source/sink and radiation. Int J Numer Meth Heat Fluid Flow 23(4):598–612

10. Parsa AB, Rashidi MM, Hayat T (2013) MHD boundary-layer flow over a stretching surface with internal heat generation or absorption. Heat Transf Asian Res 42(6):500–514

11. Mustafa M, Khan JA, Hayat T, Alsaedi A (2015) Boundary layer flow of nanofluid over a nonlinearly stretching sheet with convective boundary condition. IEEE Trans Nanotechnol 14:159–168

12. Mustafa M, Khan JA, Hayat T, Alsaedi A (2015) Analytical and numerical solutions for axisymmetric flow of nanofluid due to non-linearly stretching sheet. Int J Non Linear Mech. doi:10.1016/j.ijnonlinmec.2015.01.005

13. Raptis A (1998) Radiation and free convection flow through a porous medium. Int Commun Heat Mass Transf 25:289

14. Nayak MK, Dash GC, Singh LP (2015) Unsteady radiative MHD free convective flow and mass transfer of a viscoelastic fluid past an inclined porous plate. Arabian J Sci Eng. doi:10.1007/s13369-015-1805-8

15. Cortell R (2007) MHD flow and mass transfer of an electrically conducting fluid of second grade in a porous medium over a stretching sheet with chemically reactive species. Chem Eng Process 46(8):721–728

16. Cortell R (2008) Effect of viscous dissipation and radiation on the thermal boundary layer over a nonlinearly stretching sheet. Phys Lett Sect A 372(5):631–636

17. Singh AK (2008) Heat source and radiation effects on magneto-convection flow of a viscoelastic fluid past a stretching sheet: analysis with Kummer's functions. Int Commun Heat Mass Transf 35:637–642

18. Chen Chien-Hsin (2010) On the analytic solution of MHD flow and heat transfer for two types of viscoelastic fluid over a stretching sheet with energy dissipation, internal heat source and thermal radiation. Int J Heat Mass Transf 53:4264–4273

19. Chakrabarti A, Gupta AS (1979) Hydromagnetic flow and heat transfer over a stretching sheet. Q Appl Math 37:73–78

20. Liu I-C (2004) Flow and heat transfer of an electrically conducting fluid of second grade over a stretching sheet subject to a transverse magnetic field. Int J Heat Mass Transf 47:4427–4437

21. Datti PS, Prasad KV, Abel MS, Joshi A (2004) MHD viscoelastic fluid flow over a non-isothermal stretching sheet. Int J Eng Sci 42:935–946